Data Repository Materials for Mason et al., Dune mobility and aridity at the desert margin of northern China at a time of peak monsoon strength in the early Holocene: Methods and Geochronological Data.

All OSL and radiocarbon ages are listed below, in Tables DR1 and DR2. Study site locations are listed in Table DR3.

OSL dating methods

Methods used at the University of Nebraska-Lincoln (sample number prefix UNL, 79 of 96 samples) are described here. Methods used at Peking University (PKU, 14 samples) and Nanjing University (NJU, 3 samples) were similar, with exceptions as noted.

Sample Preparation/Dose-Rate Determination. Sample preparation was carried out under amber-light conditions. Samples were wet sieved to extract the 90 – 150 μm fraction, and then treated with 1 N HCl to remove carbonates. Quartz and feldspar grains were extracted by flotation using a 2.7 gm cm^{-3} sodium polytungstate solution, then treated for 75 minutes in 48% HF, followed by 30 minutes in 47% HCl (PKU samples did not receive this acid treatment). The sample was then resieved and the <90 μm fraction discarded to remove residual feldspar grains. The etched quartz grains were mounted on the innermost 2 mm or 5mm of 1 cm aluminum disks using Silkospray. Chemical analyses were carried out by Chemex Labs, Inc., Sparks, NV, using a combination of ICP-MS and ICP-AES (PKU sample chemical analyses used neutron activation analysis). Dose-rates were calculated using Adamiec and Aitken (1998) and Aitken (1998). The cosmic contribution to the dose-rate is determined using Prescott and Hutton (1994). For the PKU and NJU samples, these calculations were carried out using a computer program developed by R. Grün (2003)

Optical Measurements and Age Determination: Optically stimulated luminescence analyses were carried out on a Riso Automated OSL Dating System Model TL/OSL-DA-15B/C, equipped with blue and infrared diodes, using the Single Aliquot Regenerative Dose (SAR) technique (Murray and Wintle, 2000). All D_e values were determined using the Central Age Model (Galbraith et al., 1999), unless data analysis indicated partial bleaching, in which case the Minimum Age Model (Galbraith et al., 1999)was used. Preheat and cutheat temperatures were based upon preheat plateau tests between 180º and 280ºC. Dose-recovery and thermal transfer tests were conducted as described by Murray and Wintle (2003). The results of these tests for Otindag dunefield samples are described in detail by Zhou et al. (2008). Growth curves were examined to determine whether the samples are below saturation ($D/D_o < 2$; Wintle and Murray, 2006). Individual aliquots were monitored for insufficient count-rate, poor quality fits (i.e. large error in the equivalent dose, D_e), poor recycling ratio, strong medium *vs.* fast component, and detectable feldspar. Aliquots deemed unacceptable based upon these criteria were discarded from the data set prior to averaging. Averaging was carried out using the Central Age Model (Galbraith et al., 1999) unless the D_e distribution (asymmetric distribution; skew > $2\sigma_c$; Bailey and Arnold, 2006), indicated that the Minimum Age Model (Galbraith et al., 1999) was more appropriate.

FOAM Model and NCEP Data Sources.

FOAM 1.0 is a fully coupled ocean-atmosphere model that has been used to simulate Holocene climates, including changes in the global monsoons; those experiments and the model itself are described in detail by Liu et al. (2004; 2003). Monthly and seasonal means of output variables from those experiments, used to produce Figure 3, are available from the University of Wisconsin-Madison Center for Climatic Research (http://ccr.aos.wisc.edu/ , accessed May, 2008). The data used were from model runs 11k, 6k, and 0k (modern control, with pre-industrial atmospheric CO_2), all with sea-surface temperatures derived from a fully interactive ocean. Results from fixed sea-surface temperature experiments (also available from the UW-Madison Center for Climatic Research) yield patterns similar to the full-ocean results used in Figure 3. NCEP Reanalysis data (Kalnay et al., 1996) were obtained from the Earth System Research Laboratory of the National Oceanic and Atmospheric Administration, U.S. Department of Commerce (http://www.cdc.noaa.gov/cdc/data.ncep.reanalysis.html, accessed May, 2008). We used NCEP monthly long-term means (1968-1996). Gridded data from FOAM and NCEP were contoured for plotting in Figure 3.

Figure DR1. Calculation of change in potential evapotranspiration with warmer summer temperatures at 11 ka. Calculations made using the Thornthwaite equation (Thornthwaite, 1948) for two locations representing high and low values of estimated PE change in the study area: 1) Abag Qi, Otindag dunefield (A, B); and 2) Otog Qi, Mu Us dunefield (C, D). Observed monthly mean temperatures (triangles) were approximated by sine waves (solid black lines). To approximate greater seasonality at 11 ka, wave amplitudes were increased, to yield average summer (June-July-August) temperatures 4° C warmer than modern (solid gray lines). Resulting 11 ka temperatures were then used to calculate PE, with appropriate latitude adjustment for each station. PE increase is greater at Otog Qi because of higher initial temperatures.

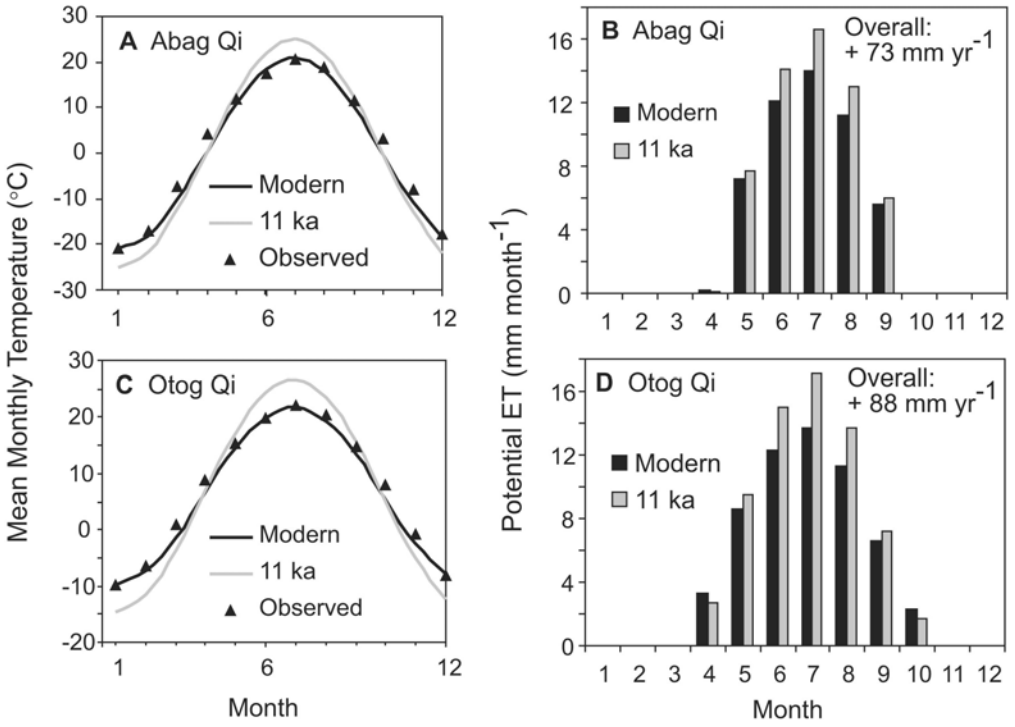

References

Adamiec, G., and Aitken, M., 1998, Dose-rate conversion factors: update: Ancient TL, v. 16, p. 37-50.

Aitken, M.J., 1998, An Introduction to Optical Dating: The Dating of Quaternary Sediments by the Use of Photon-Stimulated Luminescence: Oxford, Oxford University Press, 267 p.

Bailey, R.M., and Arnold, L.J., 2006, Statistical modeling of single grain quartz De distributions and an assessment of procedures for estimating burial dose: Quaternary Science Reviews, v. 25, p. 2475-2502.

Galbraith, R.F., Roberts, R.G., Laslett, G.M., Yoshida, H., and Olley, J.M., 1999, Optical dating of single and multiple grains of quartz from Jinmium Rock Shelter, Northern Australia: Part I, experimental design and statistical models.: Archaeometry, v. 41, p. 339-364.

Grun, R., 2003, Age.exe, computer program for the calculation of luminescence ages. Unpublished Computer Program: Canberra, Australia.

Kalnay, E., Kanamitsu, M., Kistler, R., Collins, W., Deaven, D., Gandin, L., Iredell, M., Saha, S., White, G., Woollen, J., Zhu, Y., Chelliah, M., Ebisuzaki, W., Higgins, W., Janowiak, J., Mo, K.C., Ropelewski, C., Wang, J., Leetmaa, A., Reynolds, R., Jenne, R., and Joseph, D., 1996, The NCEP/NCAR 40-Year Reanalysis Project: Bulletin of the American Meteorological Society, v. 77, p. 437-471.

Liu, Z., Harrison, S.P., Kutzbach, J., and Otto-Bliesner, B., 2004, Global monsoons in the mid-Holocene and oceanic feedback: Climate Dynamics, v. 22, p. 157-182.

Liu, Z., Otto-Bliesner, B., Kutzbach, J., Li, L., and Shields, C., 2003, Coupled climate simulation of the evolution of global monsoons in the Holocene: Journal of Climate, v. 16, p. 2472-2490.

Lu, H.Y., Miao, X.D., Zhou, Y.L., Mason, J., Swinehart, J., Zhang, J.F., Zhou, L.P., and Yi, S.W., 2005, Late Quaternary aeolian activity in the Mu Us and Otindag dune fields (north China) and lagged response to insolation forcing: Geophysical Research Letters, v. 32.

Murray, A.S., and Wintle, A.G., 2000, Luminescence dating of quartz using an improved single-aliquot regenerative-dose protocol: Radiation Measurements, v. 32, p. 57-73.

Murray, A.S., and Wintle, A.G., 2003, The single aliquot regenerative dose protocol: potential for improvements in reliability: Radiation Measurements, v. 37, p. 377-381.

Prescott, J.R., and Hutton, J.T., 1994, Cosmic ray contributions to dose rates for luminescence and ESR dating: large depths and long-term time variations: Radiation Measurements, v. 23, p. 497-500.

Stuiver, M., and Reimer, P. J., 1993, Extended 14C database and revised CALIB radiocarbon calibration program: Radiocarbon v. 28**,** p. 1022-1030.

Reimer, P. J., Baillie, M. G. L., Bard, E., Bayliss, A., Beck, J. W., Bertrand, C. J. H., Blackwell, P. G., Buck, C. E., Burr, G. S., Cutler, K. B., Damon, P. E., Edwards, R. L., Fairbanks, R. G., Friedrich, M., Guilderson, T. P., Hogg, A. G., Hughen, K. A., Kromer, B., McCormac, F. G., Manning, S. W., Ramsey, C. B., Reimer, R. W., Remmele, S., Southon, J. R., Stuiver, M., Talamo, S., Taylor, F. W., van der

Plicht, J., and Weyhenmeyer, C. E., 2004, IntCal04 Terrestrial radiocarbon age calibration, 26-0 ka BP: Radiocarbon v. 46**,** p. 1029-1058.

Thornthwaite, C., 1948, An approach toward rational classification of climate: Geographical Review, v. 38, p. 55-94.

Wintle, A.G., and Murray, A.S., 2006, A review of quartz optically stimulated luminescence characteristics and their relevance in single-aliquot regeneration dating protocols: Radiation Measurements, v. 41, p. 369-391.

Zhou, Y.L., Lu, H.Y., Mason, J., Miao, X.D., Swinehart, J.B., and Goble, R.J., 2008, Optically stimulated luminescence dating of aeolian sand in the Otindag dune field and Holocene climate change: Science in China Series D-Earth Sciences, v. 51, p. 837-847.

Table DR1. Optically stimulated luminescence ages and supporting data

Lab. Number	Site[a]	Depth (m)	H_2O (%)	K_2O (%)	U (ppm)	Th (ppm)	Cosmic (Gy/ka)	Dose Rate (Gy/ka)	D_e (Gy)	Ali-quots	Age (ka)	Context[b]
Mu Us Dunefield[c]												
UNL-679	Dabianyao	0.3	2.8	2.43	1.4	9.0	0.22	3.04±0.16	22.5±0.5	26	7.39±0.48	soil
UNL-680	Dabianyao	0.9	0.9	2.75	0.7	3.6	0.2	2.78±0.17	35.2±1.8	23	12.7±1.1	sand
UNL-681	Dabianyao	1.5	1.5	2.51	0.8	4.1	0.19	2.62±0.16	35.8±2.3	23	13.7±1.5	sand
UNL-682	Dabianyao	2.2	2.6	2.11	1.4	8.2	0.17	2.70±0.14	101.5±4.1	23	37.7±2.8	loess
UNL-683	Dabianyao	3.1	1.6	2.31	1.1	6.2	0.15	2.65±0.15	139.2±6.0	26	52.5±4.0	sand
UNL-684	Dabianyao	3.8	2.4	2.29	0.9	5.7	0.14	2.51±0.15	143.4±7.7	20	57.1±4.8	sand
UNL-904	Zhenbeitai	5.5	6.9	2.16	1.5	7.9	0.11	2.55±0.14	47.6±1.1	25	18.7±1.3	loess
UNL-905	Zhenbeitai	4.5	2.1	2.84	0.4	2.2	0.12	2.57±0.18	22.5±0.7	21	8.74±0.70	sand
UNL-906	Zhenbeitai	3.3	3.5	2.71	0.5	2.7	0.14	2.50±0.17	18.1±0.5	37	7.25±0.56	sand
UNL-907	Zhenbeitai	2.3	4.4	2.82	0.6	3.2	0.16	2.58±0.17	6.9±0.2	25	2.67±0.21	sand
UNL-908	Zhenbeitai	1.0	2.1	2.69	0.8	5.5	0.19	2.85±0.17	2.7±0.1	31	0.95±0.07	sand
UNL-909	Shimao	2.1	3.2	2.51	0.7	3.4	0.16	2.47±0.16	28.5±0.6	29	11.6±0.8	sand
UNL-910	Shimao	0.5	3.4	2.58	0.7	4.1	0.2	2.61±0.16	13.3±0.3	30	5.09±0.37	sand
UNL-911	Shenshugou	2.8	3.9	2.27	1.0	5.7	0.15	3.49±0.14	26.1±0.4	40	10.5±0.7	sand
UNL-912	Shenshugou	0.7	4.7	2.31	1.2	7.3	0.2	3.71±0.15	19.6±1.7	32	7.23±0.46	soil
UNL-913	Shenshugou	0.2	1.1	2.10	1.9	10.1	0.22	3.02±0.16	0.3±0.0	23	0.11±0.01	sand
PKU-L209	Sidaogou	0.4	1.3	2.96	1.4	6.7	0.23	3.5±0.1	26.3±1.7	12	7.56±0.58	soil
PKU-L210	Sidaogou	0.8	0.9	2.74	1.4	5.6	0.22	3.2±0.1	25.8±1.4	18	8.10±0.57	soil
PKU-L211	Sidaogou	1.6	1.3	3.01	1.1	5.4	0.19	3.3±0.2	27.7±1.3	17	8.38±0.55	soil
PKU-L212	Sidaogou	2.2	2.3	2.34	1.0	4.8	0.18	2.5±0.1	24.6±0.9	42	9.78±0.63	sand
PKU-L213	Sidaogou	2.8	1.9	2.42	0.9	4.1	0.17	2.5±0.1	27.6±1.6	24	11.0±0.8	sand
PKU-L214	Sidaogou	3.2	4.4	2.54	2.2	11.1	0.16	3.4±0.1	140.4±7.2	12	41.8±2.6	loess
PKU-L215	Caijiagou	0.4	6.2	2.74	1.2	7.1	0.22	3.1±0.1	22.5±0.5	18	7.29±0.33	soil
PKU-L216	Caijiagou	0.8	0.8	2.68	1.1	5.8	0.21	3.0±0.1	23.5±1.1	18	7.81±0.50	soil

PKU-L217	Caijiagou	1.3	0.3	2.45	1.2	5.5	0.20	2.9±0.1	24.4±0.9	12	8.55±0.48	sand
PKU-L218	Caijiagou	2.2	1.3	2.58	0.7	3.3	0.17	2.6±0.1	25.7±0.8	29	9.98±0.61	sand
Otindag Dunefield[d]												
UNL 1222	Sangan Dalai North	0.5	0.7	2.65	0.5	2.0	0.23	2.68±0.10	0.35±0.02	25	0.13±0.01	sand
UNL 1223	Sangan Dalai North	1.4	0.5	2.53	0.5	2.0	0.20	2.56±0.10	1.61±0.06	17	0.63±0.04	sand
UNL 1224	Sangan Dalai North	3.0	2.4	2.41	0.5	2.1	0.16	2.35±0.09	1.61±0.06	20	0.68±0.04	sand
UNL 1225	Sangan Dalai North	5.65	0.5	2.89	0.4	1.9	0.12	2.75±0.11	11.12±0.24	18	4.04±0.22	soil
UNL 1226	Sangan Dalai North	7.35	2.8	2.65	0.4	1.5	0.10	2.43±0.09	24.01±0.65	26	9.90±0.55	sand
UNL 1821	Sangan Dalai North	5.9	0.6	2.48	1.0	3.6	0.12	2.65±0.10	112.0±0.4	23	4.52±0.27	soil
UNL 1847	Sangan Dalai North	6.4	1.2	2.32	0.4	1.8	0.11	2.23±0.09	21.25±0.46	21	9.51±0.53	sand
UNL 1227	New Hwy 207 Km 116	6.0	2.8	2.29	0.5	2.0	0.11	2.21±0.09	1.39±0.03	18	0.63±0.04	sand
UNL 1228	New Hwy 207 Km 116	8.0	2.3	2.29	0.5	2.1	0.09	2.21±0.09	1.39±0.04	20	0.63±0.04	sand
UNL 1229	Sangan Dalai South A	2.0	3.8	2.77	0.6	2.4	0.18	2.69±0.10	1.16±0.06	17	0.43±0.03	sand
UNL 1230	Sangan Dalai South A	2.65	3.0	2.77	0.5	2.1	0.17	2.66±0.10	1.75±0.05	17	0.66±0.04	sand
UNL 1231	Sangan Dalai South A	3.6	3.9	2.65	0.5	2.1	0.15	2.51±0.10	3.26±0.13	33	1.30±0.07	sand
UNL 1232	Sangan Dalai South A	5.6	12.0	2.77	0.8	3.6	0.12	2.52±0.11	21.00±0.35	18	8.33±0.46	sand
UNL 1233	Hwy 303 Km 55	3.0	3.6	2.53	0.5	2.2	0.16	2.44±0.09	3.96±0.13	23	1.62±0.09	sand
UNL 1234	Hwy 303 Km 55	4.5	3.0	2.65	0.5	2.4	0.14	2.55±0.10	22.15±0.48	18	8.68±0.47	sand
UNL 1235	Hwy 303 Km 55	8.0	1.6	2.17	0.5	2.4	0.09	2.16±0.08	20.22±0.37	19	9.37±0.50	sand
UNL 1236	Jing Peng E	1.0	1.6	2.41	0.5	2.5	0.20	2.46±0.09	4.91±0.12	23	1.99±0.11	sand
UNL 1237	Jing Peng E	2.3	3.6	2.05	0.4	1.9	0.17	2.03±0.08	5.58±0.11	18	2.75±0.15	sand
UNL 1238	Jing Peng E	3.4	3.6	1.81	0.5	2.1	0.15	1.84±0.07	6.07±0.13	32	3.39±0.17	sand
UNL 1239	Jing Peng E	4.5	4.7	2.53	0.6	2.7	0.13	2.44±0.10	3.78±0.10	17	1.55±0.09	sand
UNL 1240	Jing Peng E	9.0	6.5	1.93	0.5	2.0	0.12	1.85±0.07	2.24±0.05	31	1.21±0.07	sand
UNL 1241	Liuwangcun	0.7	1.6	2.89	0.8	5.1	0.22	3.13±0.11	13.94±0.23	26	4.46±0.22	soil
UNL 1242	Liuwangcun	2.0	3.3	2.65	0.8	4.7	0.18	2.82±0.11	22.45±0.42	17	7.96±0.42	sand
UNL 1243	Hwy 207 Km 87	8.5	7.7	3.37	0.5	2.0	0.09	2.89±0.11	6.75±0.10	25	2.34±0.12	sand

UNL 1244	Hwy 207 Km 87	9.5	4.2	3.13	0.4	1.9	0.08	2.79±0.11	13.84±0.29	17	4.97±0.27	sand
UNL 1245	Hwy 207 Km 87	14.0	3.7	3.01	0.5	1.8	0.05	2.70±0.11	14.14±0.28	16	5.24±0.28	sand
UNL 1246	Hwy 207 Km 87	15.3	3.7	3.25	0.5	2.0	0.05	2.90±0.11	19.27±0.45	20	6.64±0.37	sand
UNL 1247	Hwy 207 Km 87	20.3	2.4	3.01	0.5	1.9	0.03	2.73±0.11	24.22±0.42	17	8.88±0.47	sand
UNL 1248	Hwy 308 Km 132	0.6	1.3	2.53	0.9	4.3	0.22	2.82±0.11	2.08±0.03	19	0.74±0.04	sand
UNL 1249	Hwy 308 Km 132	1.6	5.3	2.65	0.9	4.5	0.19	2.77±0.11	2.64±0.04	19	0.95±0.05	sand
UNL 1250	Jing Peng Highway	8.5	3.2	3.13	0.5	2.0	0.08	2.85±0.11	23.38±0.45	18	8.21±0.44	sand
UNL 1835	Jing Peng Highway	3.0	1.8	2.93	0.5	2.3	0.16	2.81±0.11	0.28±0.03	62	0.10±0.01[e]	sand
UNL 1826	Jing Peng Highway	9.5	1.0	2.84	0.5	2.1	0.08	2.67±0.10	22.74±0.58	27	8.51±0.49	sand
PKU-L219	Hunshundake	0.4	0.5	3.05	0.6	2.8	0.25	3.46±0.1	0.5±0.0	12	0.14±0.01	sand
PKU-L220	Hunshundake	0.8	0.4	2.83	0.7	3.6	0.23	3.32±0.1	9.1±0.2	12	2.70±0.11	soil
PKU-L221	Hunshundake	1.8	1.1	2.81	0.8	3.5	0.20	3.30±0.1	16.7±1.1	12	5.02±0.38	soil
PKU-L222	Hunshundake	2.3	1.1	2.66	0.5	2.9	0.19	3.1±0.1	23.7±0.6	12	7.73±0.36	sand
Horqin Dunefield[f]												
UNL-1253	Baxiantong N	5.4	6.5	2.49	0.8	3.7	0.10	2.36±0.15	7.43±0.90	20	3.15±0.24	soil
UNL-1254	Baxiantong N	6.8	1.9	2.02	0.4	1.7	0.09	1.87±0.13	19.32±2.65	23	10.3±0.8	sand
UNL-1256	Sanjianzi	1.9	5.1	2.87	0.8	4.0	0.16	2.77±0.18	2.09±0.11	16	0.76±0.05	sand
UNL-1257	Sanjianzi	3	7.2	2.96	0.8	4.6	0.14	2.78±0.18	54.38±6.84	20	19.6±1.5	sand
UNL-1259	Bahuta B	9.3	4.9	2.53	0.4	2.0	0.07	2.19±0.15	22.34±3.12	19	10.2±0.8	sand
UNL-1261	Shalilai	15.8	11.2	2.43	0.3	1.6	0.04	1.90±0.15	20.55±1.73	18	10.8±0.9	sand
Tengger Desert[f]												
UNL 1832	Huanghuatan	0.6	0.8	2.24	1.5	7.5	0.24	2.97±0.12	40.82±1.53	22	13.7±0.9	sand
UNL 1827	Huanghuatan	1.9	1.8	1.93	1.4	7.1	0.20	2.59±0.11	31.06±1.91	20	12.0±1.0	sand
UNL 1823	Huanghuatan	3.3	1.8	0.07	0.2	1.0	0.15	0.33±0.03	34.84±0.73	20	106±11	sand
UNL 1841	Huanghuatan B	0.6	2.4	2.85	2.5	12.4	0.23	3.99±0.18	11.39±0.99	24	2.86±0.29	loess
UNL 1838	Huanghuatan B	1.8	1.2	2.25	1.6	8.7	0.20	2.98±0.13	25.92±1.00	20	8.56±0.55	loess

UNL 1830	Huanghuatan B	2.8	0.9	2.11	2.0	8.8	0.18	3.00±0.13	28.97±0.78	21	9.65±0.57	loess
UNL 1842	Huanghuatan B	3.8	0.6	2.00	1.2	6.4	0.16	2.55±0.11	26.99±0.71	20	10.6±0.6	sand
UNL 1825	Hwy SZ218 Km 22.3	0.4	0.5	2.06	1.5	4.1	0.21	2.57±0.10	16.47±0.68	23	6.42±0.42	sand
UNL 1846	Hwy SZ218 Km 22.3	0.7	0.6	1.90	1.0	3.2	0.21	2.23±0.09	15.02±0.65	21	6.73±0.44	sand
UNL 1836	Hwy SZ218 Km 22.3	0.4	0.5	2.02	1.1	3.3	0.21	2.38±0.09	15.76±0.59	20	6.63±0.41	sand
UNL 1828	Hwy SZ218 Km 22.3	0.5	0.6	2.05	1.2	3.9	0.21	2.47±0.10	17.38±0.74	21	7.04±0.46	sand
UNL 1822	YLH-Km 23 B	0.4	0.7	1.87	1.5	7.4	0.22	2.63±0.11	18.85±1.03	20	7.16±0.54	sand[g]
UNL 1833	YLH-Km 23 B	1.0	0.6	2.54	1.2	4.8	0.20	2.91±0.12	20.21±1.14	20	6.93±0.52	sand[g]
UNL 1834	YLH-Km 23 B	1.2	2.7	2.64	1.3	5.0	0.23	2.98±0.12	22.16±0.87	20	7.42±0.47	sand[g]
UNL 1844	YLH-Km 23 B	1.4	3.8	2.54	1.7	6.5	0.19	3.03±0.12	23.65±1.32	21	7.81±0.59	sand[g]
UNL 1850	YLH-Km 23 B	1.7	2.3	2.71	1.0	3.6	0.19	2.85±0.11	27.49±0.83	21	9.66±0.56	sand[g]
UNL 1831	YLH-Km 23 B	2.6	17.7	2.57	0.7	3.4	0.17	2.22±0.11	23.87±1.00	21	10.7±0.8	sand[g]
UNL 1824	Hwy X751 Km 128	0.3	2.0	1.94	1.5	6.9	0.21	2.62±0.11	1.06±0..09	20	0.40±0.04[e]	sand
UNL 1849	Hwy X751 Km 128	1.8	1.1	1.96	1.7	4.5	0.19	2.51±0.11	95.75±4.08	20	38.1±2.5	sand[g]
UNL 1851	Hwy X751 Km 128	2.8	1.9	1.81	1.0	4.2	0.17	2.15±0.09	98.56±4.70	20	45.8±3.2	sand[g]
UNL 1837	Babusha	1.5	0.9	1.83	1.4	6.6	0.20	2.51±0.11	1.25±0.23	24	0.50±0.10[e]	sand
UNL 1848	Babusha	2.2	1.0	1.83	1.3	7.0	0.18	2.49±0.11	0.89±0.87	27	0.31±0.15	sand
UNL 1840	Babusha	3.9	7.5	2.46	2.2	11.5	0.15	3.25±0.15	14.29±0.92	20	4.39±0.37	loess
UNL 1843	Babusha	4.5	10.0	2.93	2.6	12.5	0.14	3.65±0.17	23.92±1.50	20	6.55±0.55	loess
NJU 87	Hwy S202 Km 25	0.3	0.92	1.82	2.7	9.7		3.30±0.08	26.26±0.90	12	7.97±0.33	loess
NJU 88	Hwy S202 Km 25	0.95	0.75	1.88	2.9	10.61		3.38±0.08	32.97±1.68	6	9.77±0.55	loess
NJU 89	Hwy S202 Km 25	1.6	0.72	1.63	2.3	8.5		2.92±0.07	32.31±1.75	6	11.1±0.7	loess

a. Locations in Table DR3.
b. Sand = eolian sand with little or no pedogenic alteration; soil = surface or buried soil formed in eolian sand or loam (generally Ab horizons); loess = silt-dominated eolian sediment.
c. Mu Us dunefield ages originally reported in Lu et al. (2005); PKU ages recalculated using program of R. Grün (2003)
d. Hunshundake site ages originally reported in Lu et al. (2005) but recalculated using program of R. Grün (2003); ages UNL-1222, -1821, -1847, -1835, and -1826 are first reported in this paper; all other Otindag dunefield ages originally reported in Zhou et al. (2008).
e. Age calculated using Minimum Age Model (Galbraith et al., 1999).
f. All Horqin dunefield and Tengger desert ages first reported in this paper.
g. Intensely bioturbated fine sand; tentatively identified as eolian based on geomorphic/stratigraphic setting

Table DR2. Radiocarbon Ages

(all from soil organic matter, determined by accelerator mass spectrometry)

Lab Number	Site	Age (^{14}C yr BP)	δ^{13}C	Cal. Yr BP (95.4% prob.)[a]
AA71673	Hwy 207 Km 87	3034 ± 59	-24.5	3067-3379
AA69827	Sangan Dalai North	5396 ± 56	-25.5	6003-6084 6098-6162 6168-6294

a. Calibrated using Calib v. 5.02 (Stuiver and Reimer, 1993; Reimer et al., 2004)

Table DR3. Study Site Names and Locations

Site	Latitude (ºN)	Longitude (ºE)
Chenjiagou	38.1	109.8
Zhenbeitai	38.3	109.7
Shimao	37.9	110.0
Caijiagou	38.1	109.8
Shenshugou	38.7	110.1
Dabianyao	38.8	110.4
Liuwangcun Xi	41.4	115.0
Hwy 308 Km 132	42.4	115.4
Sangan Dalai North	42.7	115.9
Sangan Dalai South, Section A	42.7	116.0
Jing Peng Highway	42.7	116.0
New Hwy 207 Km 116	43.0	116.0
Hwy 207 Km 87	43.2	116.1
Hwy 303 Km 55	43.7	116.6
Jing Peng E	43.2	117.7
Sanjianzi	42.5	120.8
Shalilai	43.0	120.8
Baxiantong N	43.2	121.2
Bahuta B	43.2	122.2
Hwy S202 Km 25	37.4	105.2
Huanghuatan	37.5	103.4
Huanghuatan B	37.5	103.4
Hwy SZ218 Km 22.3	39.7	105.7
YLH-Km 23 B	38.6	105.5
Hwy X751 Km 128	37.5	105.0
Babusha	37.6	103.1